Check for updates

ADVANCED FUNCTIONAL MATERIALS
www.afm-journal.de

Development of a Novel Formulation of Bioactive Glass Based Calcium Phosphate Cement for Bone Grafting

Alessia D'Onofrio, Robert G. Hill, Niall W. Kent, Simon C.F. Rawlinson, and Shakeel A. Shahdad*

Particulate bone grafting material can travel from the implantation site and diminish the magnitude of required bone formation response and hence its effectiveness. An easily prepared moldable graft that rapidly sets rigid in situ would alleviate this problem and in this study, such an injectable bone graft material is presented. By combining calcium phosphate (CP) salts with a bioactive glass (BG) mixed with a 2.5% Na_2HPO_4 solution a novel BG-based calcium phosphate cement (CPC) is produced. Immersion in Tris buffer and simulated body fluid (SBF) solutions result in the rapid generation of octacalcium phosphate (OCP) and hydroxyapatite (HA) phases – a pre-requisite for "bioactivity". Cement-conditioned media does not result in any cytotoxic potential with respect to MTT activity, DNA content, or alkaline phosphatase activity with an osteoblastic cell line. Application of the cement into standardized surgical defects in the minipig mandible results in short-term, moderate irritation at 3 and 6 weeks and complete replacement of cement with new bone at 12 weeks.

1. Introduction

Bone graft substitutes are used in dentistry to promote alveolar bone preservation/augmentation following tooth loss. They represent a big portion of the global dental market size with ≈2.2 million bone graft procedures carried out annually.[1]

Bone grafts or substitutes can be obtained from different sources: autografts (derived from the same patient), allografts (derived from other humans), xenografts (from animals and other species), and alloplasts (of synthetic origin). While autografts have osteogenic, osteoinductive and osteoconductive properties that represent the ideal characteristics for a bone graft material,[2] the need for a second surgical site, low supply, and fast resorption times are some of the main drawbacks that drive the use of alternative biomaterials.[3,4]

Commercially available bone substitutes are mainly osteoconductive materials that act as scaffold for bone cell proliferation while evidence exists for the potential osteoinductive properties of allografts (although with high variability related to processing and source).[5]

Resorption times of these materials vary according to the chemical and surface characteristics of the graft and the processing during their fabrication. While xenograft, particularly the widely used deproteinized demineralized bovine bone, is a long-lasting graft with little evidence of resorption over time,[3,6] allografts and alloplasts tend to have variable resorption times from two months to several years.[3,4,7] Besides, allografts are not licensed to be sold in many countries and patients may also be hesitant to accept a bone graft from another human being. Similarly, there may be patients who would refuse animal-derived products based on their beliefs. The clinician faces the dilemma to choose appropriate biomaterials based on the required clinical application (i.e., simultaneous guided bone regeneration of bone defects and contour bone augmentation during implant surgery, socket bone grafting for alveolar ridge preservation, staged horizontal and vertical bone augmentation and maxillary sinus bone augmentation procedures). Handling properties and stability of the graft are important properties to consider: the particulate nature of the majority of these materials makes the handling and adaptation of the graft challenging in non-contained defects with higher chances of migration and instability of the graft and increased risk for wound dehiscence and reduced bone regeneration. The introduction of putty like forms and stabilization of the graft with membranes that may be tacked has somewhat reduced these risks.[8–10]

A. D'Onofrio
Centre for Oral Bioengineering
Centre for Oral Clinical Research
Institute of Dentistry
Queen Mary University of London
London E1 2AT, England
E-mail: alessia.donofrio@qmul.ac.uk
R. G. Hill, S. C. Rawlinson, S. A. Shahdad
Centre for Oral Bioengineering
Institute of Dentistry
Queen Mary University of London
London E1 2AT, England
N. W. Kent
Centre for Nature Inspired Engineering
University College of London
Gower Street, London WC1E 6BT, England

The ORCID identification number(s) for the author(s) of this article can be found under https://doi.org/10.1002/adfm.202401953

© 2024 The Authors. Advanced Functional Materials published by Wiley-VCH GmbH. This is an open access article under the terms of the Creative Commons Attribution License, which permits use, distribution and reproduction in any medium, provided the original work is properly cited.

DOI: 10.1002/adfm.202401953

16163028, 0, Downloaded from https://onlinelibrary.wiley.com/doi/10.1002/adfm.202401953 by Test, Wiley Online Library on [25/04/2024]. See the Terms and Conditions (https://onlinelibrary.wiley.com/terms-and-conditions) on Wiley Online Library for rules of use; OA articles are governed by the applicable Creative Commons License

Amongst all the available bone substitutes, deproteinized bovine bone and freeze-dried allografts dominate the market.[1] There has hardly been any innovation to develop new synthetic materials to address the deficiencies associated with existing options.

Alloplastic bone substitutes are characterized by a large group of synthetic biomaterials, including CP based materials, like CP ceramics and cements, and BGs. CP ceramics (i.e., synthetic HA $Ca_{10}(PO_4)_6(OH)_2$; beta-tricalcium phosphate β-TCP$Ca_3(PO_4)_2$ or biphasic CP, a mixture of HA and β-TCP with different ratios) that are similar in composition to the mineral phase of bone, are bioactive (i.e., promote apatite formation) and osteoconductive. BGs are silicate-based amorphous solids. The HA formed on their surface once implanted is responsible for the strong bond between the glass and the bone through interaction with collagen fibrils.[11] The main advantage of a BG is that the composition can be easily modified to alter the properties of the material. The release of critical concentrations of ionic dissolution products from the BG has been shown to have the potential to promote new bone formation by activating osteoprogenitor cells[12,13] and stimulating angiogenesis.[14,15] Antibacterial properties have also been reported for some BG compositions due to in situ release of ions and change of pH.[16] However, the rise in pH due to the dissolution and ion release has also shown to have detrimental effects. In closed system experiments, the alkalinization of the extracellular fluid (pH >7.9) can impair osteogenic differentiation of mesenchymal stem cells, in contrast with the beneficial effect obtained with moderate alkalosis (up to 7.56).[17] Osteoblast function is stimulated by a slightly alkaline environment, osteoclast function, however, is decreased impairing the initial steps of bone healing.[18] While this increase in pH is evident in the closed micro-environment of a cell culture experiment, when BG is applied in vivo in a dynamic environment where there is a continuous replacement and washout of fluids, this disadvantage may be negligible because of the internal environment homeostasis.[19–21]

The desire for faster resorbing materials, greater bone-to-graft contact, improved handling properties, and a strength that could allow for some degree of local stabilization has led to the development of CPCs.[22] They are used as bone grafts for orthopedics and craniofacial applications, while their use in dentistry is limited to applications as desensitizing agents. CPCs are produced by mixing reactive crystalline CP powders with an aqueous solution to form a self-hardening paste. During the setting reaction, depending on the pH value, the cement may form a poorly crystalline HA or dicalcium phosphate dihydrate (DCPD, brushite, $CaHPO_4.2H_2O$).[23] The major advantages of CPCs include the ability to harden in vivo at body temperature, mouldability and easy manipulation, possessing excellent osteoconductive properties, and biocompatibility. Once set, they form chemical bonds with the host bone and have a chemical composition similar to that of the mineral phase of the bone.[23] However, the resulting cement is weak under tensile forces, limiting its use to non-load bearing applications or in combination with metal implants.[24] CPCs have poor water stability, meaning they will disintegrate if not completely set.[25,26] Finally, the CP salts used as the reactive precursors are restricted in their stoichiometry, so that alterations to the physiochemical properties are limited to the salts used. CPCs are not routinely used in dental bone grafting applications although the advantage of having an in situ-setting material used as a bone graft is recognized. Calcium sulphate cements offer an in situ setting alternative to particulate graft materials. However, their resorption rate is fast which is not suitable for all clinical applications, and they suffer from poor mechanical properties.[27] Their use in dentistry as bone graft materials is limited with no robust evidence of their efficacy compared to other alloplastic and xenograft alternatives.[28]

To combine the benefits of BGs and CPCs in a unique device, the BG has been used as a reactive component of a CPC, wherein a BG powder is mixed with a CP salt and a 2.5% Na_2HPO_4 solution to form HA.[29] The BG works as a precursor by providing Ca^{2+} and PO_4^{3-} ions for the formation of HA. In the cement compositions first studied, the reaction pathway led to the formation of DCPD in the first instance, then OCP ($Ca_8(HPO_4)_2(PO_4)_4.5H_2O$) followed by HA. Importantly, by changing the glass composition, the rate of the setting reaction and the phases formed could be controlled.[29]

The advantages of using BG as a reactive precursor for the formation of a CPC are: 1) The setting rate, phases formed, and material properties can be controlled by the glass composition, with no stoichiometric and solubility restrictions as for salts used in conventional CPCs; 2) Using BG introduces the silicate phase, a site for heterogeneous nucleation leading to more rapid nucleation than conventional CPCs;[30] 3) Dissolution products like silicates and calcium have been shown to stimulate pre-osteogenic responses – collagen type I formation and osteoblastic differentiation;[31] and 4) Therapeutic ions like strontium, fluoride, zinc can be introduced in the glass composition to improve biological and physical properties of the cement.

The aims of this study were to characterize the in vitro properties of the newly developed BG-based CPC and to evaluate local alveolar bone tissue effects and performance in a minipig alveolar bone defect model. The BG based CPCs developed offer advantages compared to current bone graft materials used in dentistry with the opportunity to inject into the defect void with easy manipulation of the graft in the bone defect, in situ setting ability, and the potential for tailoring properties according to the clinical need due to the versatility of the BG.

2. Results and Discussion

In this study, the development of a novel formulation of a BG based CPC was shown where the BG acts as a reagent in the setting reaction of the CPC providing Ca^{2+} and PO_4^{3-} ions used in the formation of HA and its precursors.

In a previous study, the setting reaction of these types of cements, and the effect of changes in glass composition on the setting reaction were studied.[29] The first step in the setting reaction is the rapid dissolution of the highly soluble CP salts in solution, which creates an acidic environment. The H^+, Ca^{2+}, and PO_4^{3-} ions released during the dissolution precipitate forming DCPD, which is favored due to the acidity of the reaction solution.[32]

$$Ca(H_2PO_4)_2.H_2O + Ca(H_2PO_4)_2 + H_2O \rightarrow 2CaHPO_4.2H_2O + 2H_3PO_4 \quad (1)$$

The H_3PO_4 species produced will dissociate as below:

$$H_3PO_4 \rightarrow 3H^+ + PO_4^{3-} \quad (2)$$

© 2024 The Authors. Advanced Functional Materials published by Wiley-VCH GmbH

In an acidic environment faster degradation of the BG occurs.[33] The glass dissolves through an ion exchange between protons in solution and calcium and sodium ions in the glass network which results in an increase in pH of the solution and formation of silanol groups on the silicate layer of the glass.

$$2\,(Si-O)\,Ca + 2H^{+} \rightarrow 2SiOH + Ca^{2+} \quad (3)$$

$$R-(Si-O)\,Na + H^{+} \rightarrow R-SiOH + Na^{+} \quad (4)$$

Due to the rise in pH a dissolution/precipitation process occurs, leading to dissolution of DCPD and precipitation of OCP.

$$10CaHPO_4.2H_2O \rightarrow Ca_8(HPO_4)_2(PO_4)_4.5H_2O + 2Ca^{2+} + 4H_2PO^{4-} + 15H_2O \quad (5)$$

The time point at which this process occurs and the rate at which it happens is dependent on the glass compositions. OCP over time is transformed toward HA via a solid-state phase transition.

$$Ca_8(HPO_4)_2(PO_4)_4.5H_2O + 2(OH)^{-} + 2Ca^{2+} \rightarrow Ca_{10}(PO_4)_6(OH)_2 + 5H_2O + 2H^{+} \quad (6)$$

This process is thermodynamically driven as HA is more stable than OCP.[34]

By changing the glass composition, the rate of the setting reaction and phases formed can be controlled. In a previous study, the effect of sodium substitution for calcium in the glass composition has been investigated.[35] The setting reaction changed from DCPD→ OCP→ HA to OCP→ HA. The increase in sodium content might raise the pH during the setting reaction after the initial acidity caused by the dissolution of the salt, reaching values outside the stability range of DCPD and causing a direct precipitation of OCP.

Before moving to test the new cement formulation at a preclinical level using an animal model, it was important to characterize and test the cement produced in vitro, to assess the physical properties of the material, and to evaluate its in vitro safety on osteoblastic cell line.

2.1. In Vitro Characterization of the BG-CPC

2.1.1. Setting Time

The setting time measured for the cement (**Figure 1**) was on average 13±2 min (initial setting time) and 31 ± 2 min (final setting time).

Clinically, the cement should be implanted before the initial setting time (which indicates the end of mouldability of the paste without damage to the cement) and the wound should be closed after the final setting time (time beyond which it is possible to touch the cement without causing deformation).[36] An initial setting time between 4 and 8 min and a final setting time below 15 min are generally accepted as optimal values.[23] The experimental cement showed longer setting times compared to these recommended values. Cements from this same batch were used for the in vivo animal study and the slightly long setting time did not have a detrimental effect on the surgical procedure – instead it allowed an optimal time for handling of the material.

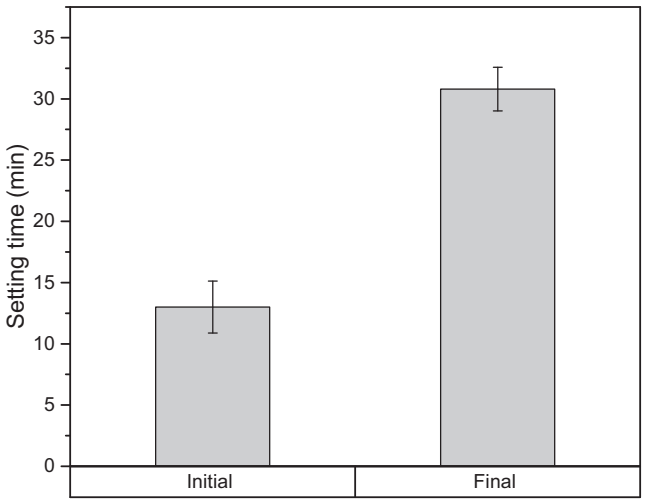

Figure 1. Initial and final setting time of cement was measured using a Gilmore needle test. Data are presented as mean ± SD, $n = 5$ measurements.

2.1.2. Phase Analysis

Following immersion in Tris buffer and SBF solutions, the formation of a mixture of OCP (ICSD ref: 00-044-0778) and HA (ICSD ref: 01-074-0565) was seen. This was limited to the 1 h and 1 day XRD patterns for cements immersed in Tris buffer, while it was present up to 28 days for cements immersed in SBF (**Figure 2**). The presence of OCP is indicated by the two diffraction lines at 4.5 and 9.9 $2\theta°$.[32] OCP is believed to be a precursor in the formation of HA: at a pH between 5.0 and 9.0, OCP will be an intermediate phase before HA formation, whereas if the reaction conditions are above pH 9.0, then HA will precipitate directly.[37] It has been argued that the reaction from OCP to HA occurs through crystal transition, rather than dissolution and reprecipitation.[38] Crystal phases in CPCs generally form via homogeneous nucleation, with the initial phase formed being the phase most kinetically favored, which is the one that requires the lowest activation energy barrier for crystal nucleation.[39] According to the Ostwald–Lussac law, the crystallization then proceeds along a series of phases until the most stable one is formed.[40] The high water content in the OCP crystal structure is likely to increase the affinity with the surrounding solution and lowers the interfacial energy which in turn favors its nucleation despite HA being the most thermodynamically stable phase.

A diffraction line characteristic for monetite at 26.5 $2\theta°$ (ICSD ref: 04-009-4184) was present at 1 h for the Tris immersion and up to 28 days in SBF. After 7 and 28 days only HA was identified in the XRD patterns of the cements immersed in Tris buffer, while a mixture of OCP/HA was present in the cements immersed in SBF. The diffraction lines at 25.9 and the triplets at 32.1, 32.6, and 33.9 $2\theta°$ increased in intensity and definition with time in both experimental conditions. The slight shift of 300 diffraction line (33.9 $2\theta°$) toward larger 2θ values compared to the reference identified for HA (32.8 $2\theta°$) might be related to the incorporation of CO_3^{2-} in the apatite structure which is known to decrease the a axis of the lattice.[41] The slower transition from OCP to HA seen in SBF can be related to the presence of Mg^{2+} in SBF

© 2024 The Authors. Advanced Functional Materials published by Wiley-VCH GmbH

16163028, 0, Downloaded from https://onlinelibrary.wiley.com/doi/10.1002/adfm.202401953 by Test, Wiley Online Library on [25/04/2024]. See the Terms and Conditions (https://onlinelibrary.wiley.com/terms-and-conditions) on Wiley Online Library for rules of use; OA articles are governed by the applicable Creative Commons License

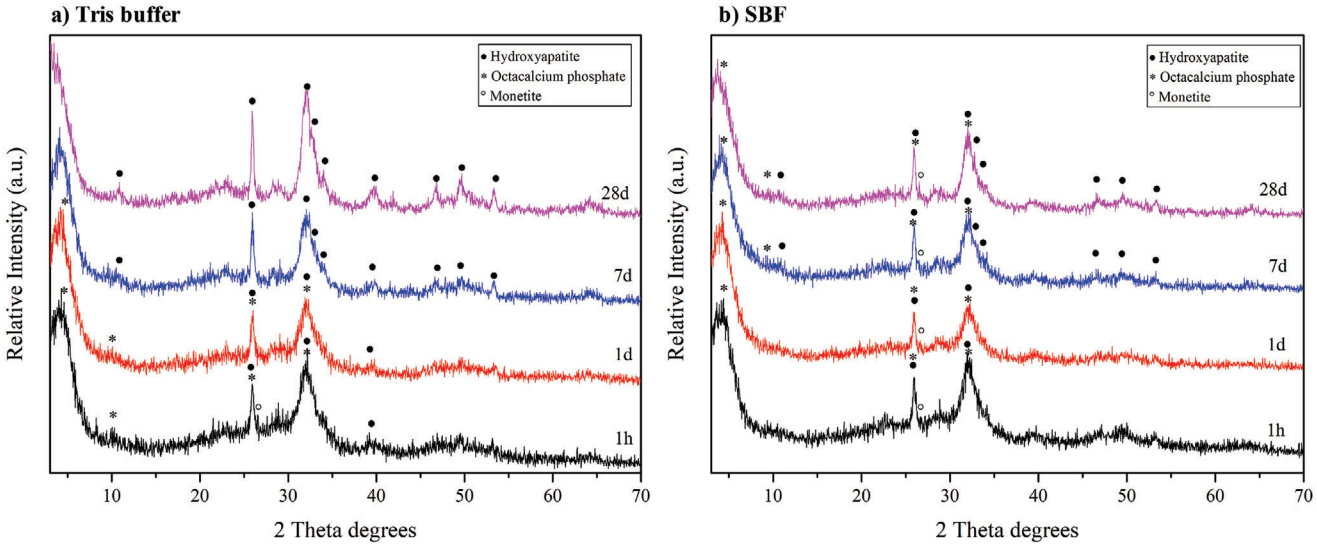

Figure 2. XRD patterns of the cement after immersion in a) Tris buffer solution and b) SBF for 1 h, 1 day, 7 days, and 28 days. * OCP; ●HA; */● indistinguishable OCP/HA; ° Monetite.

solution which is known to inhibit the hydrolysis of OCP to HA.[42] The presence of OCP, HA and CO_3^{2-} substitutions in the apatite formed were confirmed by analysis of FTIR results (Section S1, Supporting Information).

2.1.3. Compressive Strength

The maximum compressive strength was measured at 1 h in both immersion media (20.7 ± 2.8 MPa for Tris and 19.9 ± 3.1 MPa for SBF). A trend in drop of strength with increase of time of immersion was seen (**Figure 3**). Immersion in SBF resulted in higher compressive strength values maintained over time compared to Tris buffer immersion, with a drop after 1 h and similar values maintained up to 28 days. In Tris, compressive strength reduced proportionally with an increase in immersion time. The decrease in compressive strength after 1 h in both immersion solutions is believed to be due to the transition of OCP to HA, a process that is likely to cause porosity within the cement matrix. OCP is formed by alternated "apatitic" layers (with identical structure to HA) and a hydrated layer, not present in the HA. The gradual conversion of OCP to HA and loss of the hydrated layer induces porosity within the interlocked crystals in the cement matrix. As the conversion from OCP to HA is delayed in the cements immersed in SBF, less porosity forms within the cement structure, resulting in higher strength values.

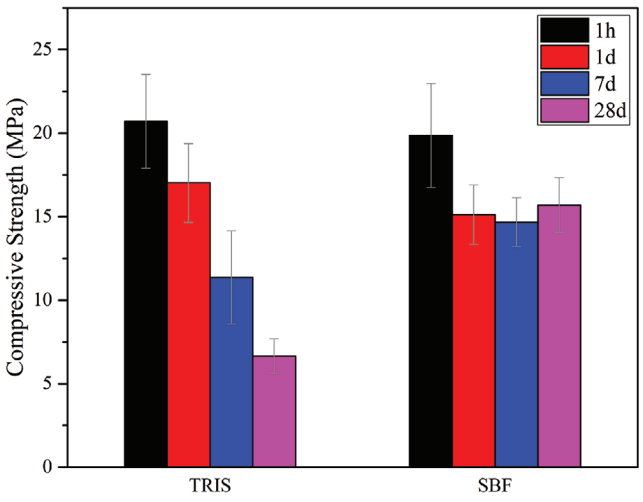

Figure 3. Compressive strength (mean± standard deviation, $n = 8$) of cement cylinders immersed in Tris buffer and SBF solutions for 1 h, 1 day, 7 days, and 28 days.

As in most clinical applications, CPCs are applied in direct contact with trabecular bone, an ideal material should match the compressive strength of the bone (8 and 13 MPa) into which it is implanted.[23] As the maximum strength obtained in both immersion media was above 19 MPa, these cements can meet this clinical requirement for non-loaded sites of bone.[43] However, the compressive strength values obtained should only be interpreted as a way of comparing the different behavior in solution and time points of the cement rather than values applicable in vivo. Many factors will affect the strength of the cement in vivo including the amount of cement, morphology of the grafted site, presence of sources of Ca^{2+} and PO_4^{-3} in body fluids, body fluid replenishment rate, and biological factors associated with osseointegration.[44] A comparison between in vitro values of compressive strength achieved in this study and those from different studies available in the literature is also difficult to undertake as different methodologies are usually used. Values reported in the literature range from 10–100 MPa.[26] The way the cement is mixed and compacted in the molds to obtain the specimen affects the porosity and therefore the strength of the material. The values obtained by applying pressure do not reflect those achieved in vivo as usually the cement is injected without applying significant condensation pressure.[45] Immersion media used for soaking the cement samples and testing conditions (wet and dry) will also affect the strength values obtained.

© 2024 The Authors. Advanced Functional Materials published by Wiley-VCH GmbH

16163028, 0, Downloaded from https://onlinelibrary.wiley.com/doi/10.1002/adfm.202401953 by Test, Wiley Online Library on [25/04/2024]. See the Terms and Conditions (https://onlinelibrary.wiley.com/terms-and-conditions) on Wiley Online Library for rules of use; OA articles are governed by the applicable Creative Commons License

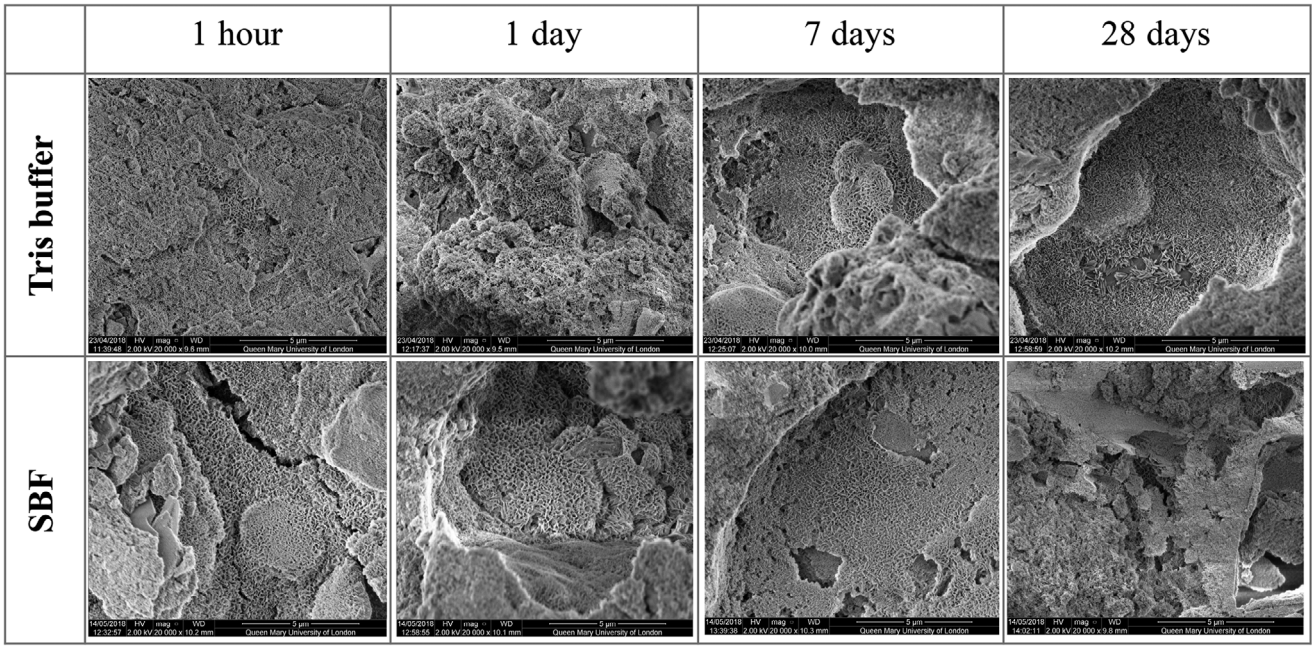

Figure 4. Scanning electron micrographs of cement after immersion in Tris buffer and SBF for 1 h, 1 day, 7 days, and 28 days.

As the strength of a cement is determined by the interlocking of the crystallites of the phases formed [46] and their shape, assessing the microstructure of the material under SEM can give a useful insight in the properties of the cement.

2.1.4. Cement Microstructure

The microstructure of the cement after immersion in Tris buffer and SBF appeared similar under SEM (**Figure 4**). At all time points, small plate-like crystals covered the fractured surfaces of the cement. The plate-like morphology reflects the formation of HA through an OCP precursor.[32]

2.1.5. Ion Release

After immersion of the cement in Tris buffer the levels of Ca^{2+} in solution were generally very low at each time point. The initial release of Ca^{2+} after 1 h was followed by its consumption at later time points. In SBF, the Ca^{2+} available in solution was gradually consumed over time. OCP transforms to HA following these two reactions, depending on the availability of Ca^{2+} ions:

$$Ca_8H_2(PO_4)_6.5H_2O + 2Ca^{2+} \rightarrow 2Ca_5(PO_4)3OH + 3H_2O + 4H^+ \quad (7)$$

$$1.25Ca_8H_2(PO_4)_6.5H_2O \rightarrow 2Ca_5(PO_4)3OH + 1.5H_3PO_4 + 4.25H_2O \quad (8)$$

Therefore, even at the very low Ca^{2+} concentrations found in Tris buffer transition from OCP to HA can occur according to Equation (8).

Both solutions showed a similar trend for P release, increasing with time up to 7 days and then slightly reducing at 28 days. This is expected as during the transition from OCP to HA P is normally released. A lower amount of P was released in SBF solution at 1 day and 7 days compared with Tris buffer (taken into account the P concentration in SBF before immersion) which is related to the delayed conversion from OCP to HA.

The Si release in Tris and SBF showed a similar trend with increased concentration in solutions over time. This is related to the progressive hydrolysis of the residual silicate chains of the glass, leading to release of soluble silicon species into solution.

A similar trend of Na^+ release was found in both immersion solutions, with an increase of Na^+ concentration over time related to the dissolution of the glass (**Figure 5**).

2.1.6. Cell Culture Studies

Osteoblast cells cultured in cement extracts showed a reduction of cell viability to 56% after 1 day for the test cement compared with the negative control (NC, non-conditioned culture medium α-MEM). However, after culture for 7 days, higher, but not significant, cell viability was recorded for the test cement compared to NC, suggesting that cells recovered, and no signs of cytotoxicity were present (**Figure 6a**). This was considered a transient cytostatic effect instead of a cytotoxic effect, with conditioned medium slowing down the initial growth of osteoblasts, without exerting a cytotoxic effect. With time, cells proliferated and metabolically reduced the tetrazolium dye to the same degree as for the cells treated with NC. Cells maintained their normal morphological phenotype when treated with NC and test cement, while cellular lysis was visible for cells exposed to SLS (Figure 6c).

Osteoblast proliferation followed the same trend seen for the MTT assay, with a lower cell number at 1 day compared to NC (data not shown) and an increase in cell proliferation after 7 days compared to NC. ALP activity measured at 7 days followed the same trend seen for cell proliferation (Figure 6b).

© 2024 The Authors. Advanced Functional Materials published by Wiley-VCH GmbH

16163028, 0, Downloaded from https://onlinelibrary.wiley.com/doi/10.1002/adfm.202401953 by Test, Wiley Online Library on [25/04/2024]. See the Terms and Conditions (https://onlinelibrary.wiley.com/terms-and-conditions) on Wiley Online Library for rules of use; OA articles are governed by the applicable Creative Commons License

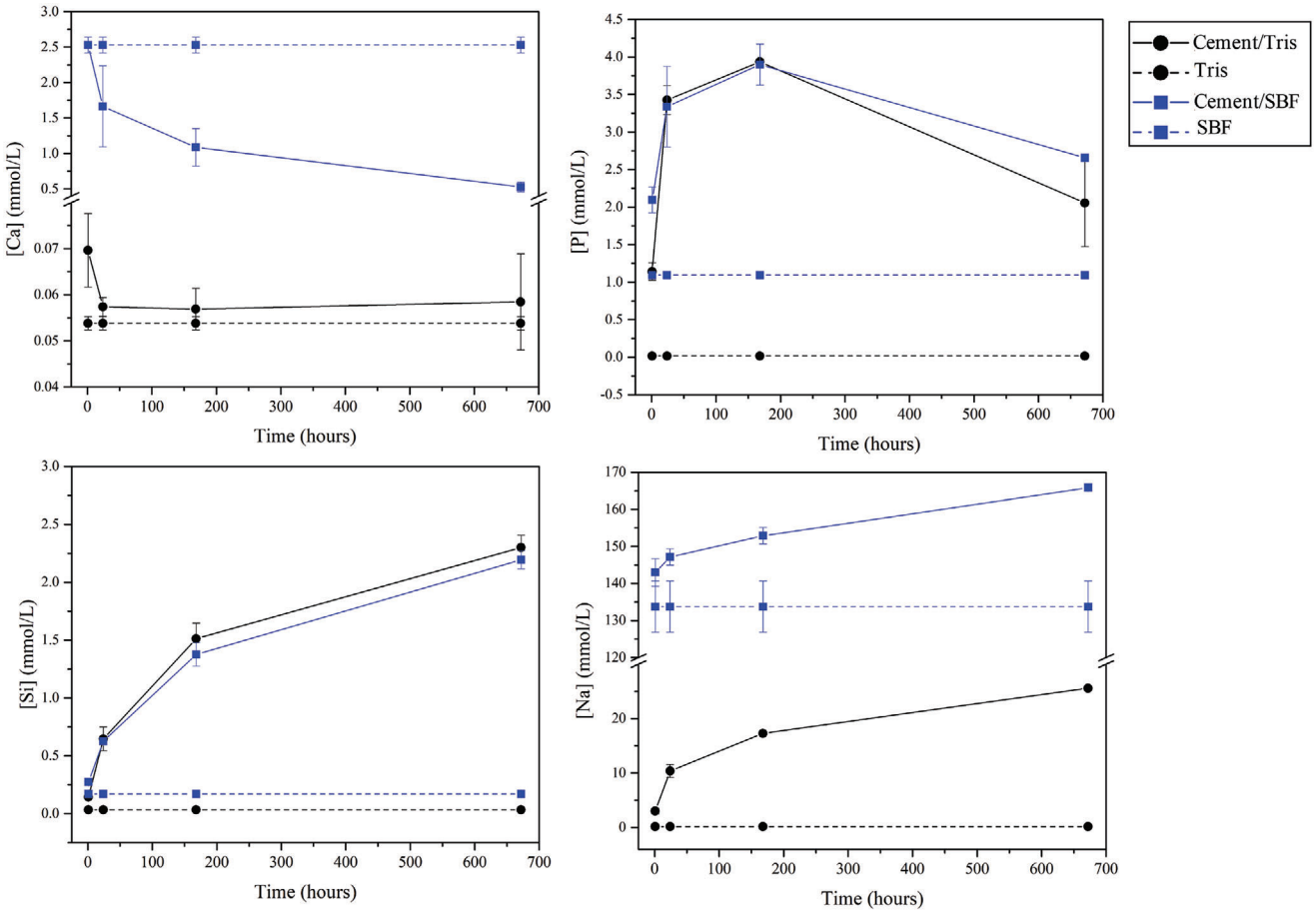

Figure 5. Elemental concentration (mmol L^{-1}) of Ca, P, Si, and Na as determined by inductively coupled plasma optical emission spectrometry (ICP-OES) after cement immersion in Tris and SBF for 1 h, 1 day, 7 days, and 28 days. The ions concentration in SBF and Tris buffer solutions as prepared are also reported for reference. Time expressed in hours. Data are presented as mean±SD, $n = 3$.

2.2. In Vivo Performance of BG Based CPC

In the present study, the in vivo performance of a new BG-CPC was analyzed for new bone formation in standardized surgical defects in minipig mandibles and compared with the performance of a i) biphasic calcium phosphate ceramic (Bone Ceramic, Straumann, BC, HA/β- TCP 60%:40% ratio) and ii) untreated defects (NC).

At 3 weeks, the cement was present in all sites grafted with the test material apart from one site (animal 325326 right side) where resorption and degeneration of host bone were visible in the grafted area (**Figure 7**). The cement was well adapted to the contour of the defect, filling the space within the trabecular structure of the cancellous host bone. New bone formation in general was low and only observed near the defect walls. A low-severity degree of fibrosis and chronic and/or purulent inflammation was found in most of the sites around the defect walls, with scalloping of areas of bone suggestive of osteoclastic resorption at Howship's lacunae.

In defects grafted with BC, new bone formation was confined to the defect walls and around the periphery of the particles. In particular, it was noted that, consistently, new bone tended to form more at the bottom and from the lingual wall of the cavity, whereas a trabecular bone structure could be identified compared to the dense cortical bone at the buccal side of the defects. Despite the self-containing nature of the defect, BC particles at the top of the defect were displaced toward the adjacent soft tissues. Areas of fibrosis were identified filling the space between the graft particles.

In the NC group after 3 weeks, new bone formation was higher compared with both test and positive control group, with more woven bone formed at the bottom and lingual side of the wall defect and extending to the center and upper part of the defect.

After 6 weeks, the BG-CPC was visible in six out of twelve sites grafted while in the remaining six sites resorption and degeneration of host bone were visible in the grafted area, with either no sign of cement or only remnants of cement present (**Figure 8**). In the sites where the cement was visible, degradation of the material was seen: a reduced defect area was occupied by the cement which presented an irregular outline with fragments and particles of degraded cement visible around the defect. New bone formation was seen in direct contact with the surface of the material, which provided a scaffold for new bone growth without loss of the vertical component of the defect. In the sites where the graft material was not visible or only small remnants were left, a moderate purulent and/or chronic inflammation was present. A moderate

© 2024 The Authors. Advanced Functional Materials published by Wiley-VCH GmbH

16163028, 0, Downloaded from https://onlinelibrary.wiley.com/doi/10.1002/adfm.202401953 by Test, Wiley Online Library on [25/04/2024]. See the Terms and Conditions (https://onlinelibrary.wiley.com/terms-and-conditions) on Wiley Online Library for rules of use; OA articles are governed by the applicable Creative Commons License

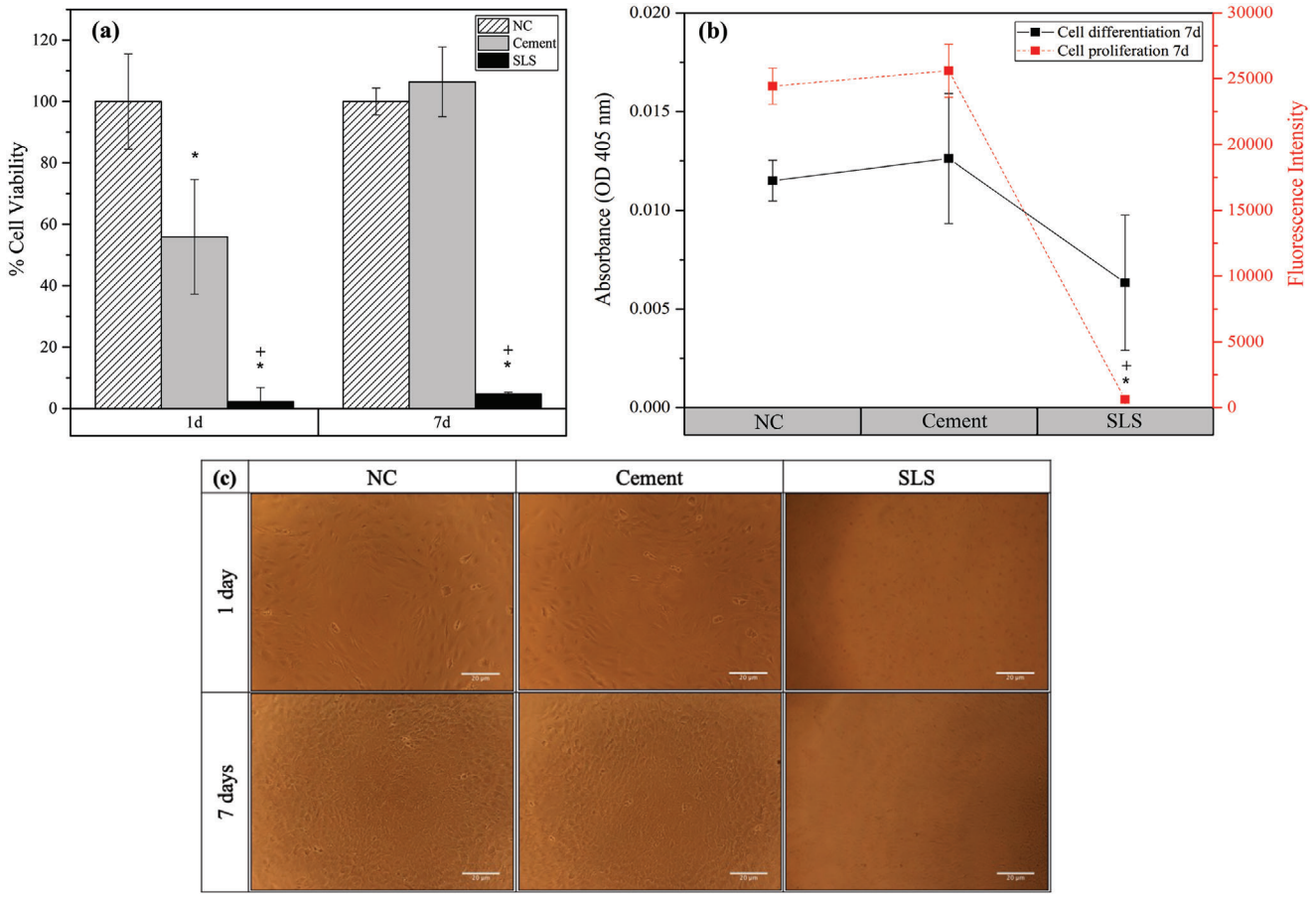

Figure 6. a) Effect of cement extracts on the viability of osteoblast cells (MC3T3-E1 cell line) measured via an MTT assay at 1 day and 7 days. Data are presented as percentages of cell viability normalized against the negative control. Error bars represent standard deviation of the mean of six wells per treatment of three independent experiments. Mann–Whitney U test used for 1 day results, unpaired *t*-test used for 7 days. $^{*}p < 0.05$ compared to NC. $+\ p < 0.05$ compared to cement. b) Effect of cement extract on the differentiation of osteoblasts measured via an ALP activity assay (left Y axis) and on their proliferation measured via a DNA assay (right Y axis) after 7 days. Error bars represent standard deviation of the mean of six wells per treatment of three independent experiments. Unpaired *t*-test used for statistical analysis. $^{*}p < 0.05$ compared to NC. $+\ p < 0.05$ compared to cement. c) Osteoblast morphology as observed under light microscope 1 day and 7 days Scale bar:20 μm. NC: negative control, non-conditioned culture medium; SLS: positive control, 0.1 mg ml^{-1} solution of sodium lauryl sulphate in α-MEM.

bone degeneration with loss of normal structure and clumping of osteoid and a moderate degree of fibrosis within the defect area were visible. The defect area in some sites was enlarged compared to the initial defect, possibly due to a rapid degeneration and resorption of bone adjacent to the defect walls.

Sites grafted with BC showed an increased level of new bone formation within the defect area, around the particles, and within the intergranular space, compared to the 3 week results. No signs of fibrosis or inflammatory reaction were present at this time and no evident signs of resorption of the particles could be noticed.

After 6 weeks the NC sites showed an almost complete filling of the defect area with new woven bone and with the defect walls still recognizable.

At 12 weeks only one site showed the presence of the test cement (**Figure 9**), while all the other grafted sites were clear of residual cement in the defect. The remodeled site was much larger than the original defect site and was filled with new woven bone. In three samples signs of bone degeneration, fibrosis or inflammation were present.

Sites grafted with BC after 12 weeks showed no sign of inflammatory reaction and an increased amount of new bone formed within the particles filling the center of the defect. In some cases, the particles in the most coronal portion of the defect showed signs of encapsulation in soft tissue. No signs of evident particle resorption was seen.

The NC sites showed an almost complete filling of the defect area with new woven bone and bone marrow and no signs of inflammatory reaction.

Semi-quantitative histopathological analysis (Section S2, Supporting Information) showed that at 3 weeks all the groups induced a slight reaction of the surrounding tissues, with the highest score recorded for NC. This initial reaction was expected as consequence of the surgical trauma and subsequent initiation of the healing process.[47] These responses reflect the normal fracture repair process of the granulation tissue formation phase where platelet-derived growth factor (PDGF) and transforming growth factor β (TGF-β) act to initiate an inflammatory response with subsequent promotion of repair processes.[48] However, an

© 2024 The Authors. Advanced Functional Materials published by Wiley-VCH GmbH

16163028, 0, Downloaded from https://onlinelibrary.wiley.com/doi/10.1002/adfm.202401953 by Test, Wiley Online Library on [25/04/2024]. See the Terms and Conditions (https://onlinelibrary.wiley.com/terms-and-conditions) on Wiley Online Library for rules of use; OA articles are governed by the applicable Creative Commons License

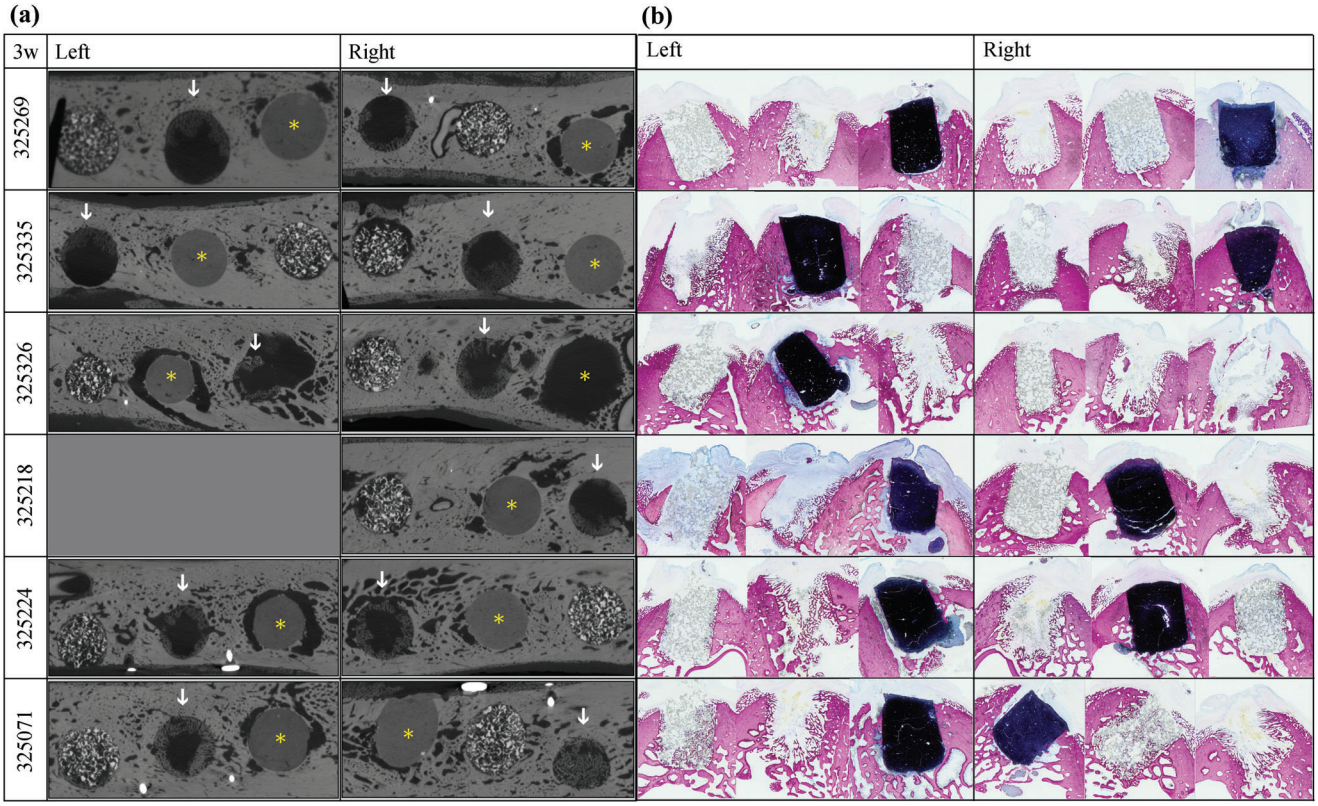

Figure 7. a) Axial view of XMT of samples at 3 weeks divided by left and right side of the mandible. Yellow asterisk: test cement; white arrow: NC; sites filled with particulate radiodense material (not marked): BC. b) Correspondent histological images of buccal lingual sections. Each animal is identified by a unique number (on the left column).

important difference was noted when cellular response and tissue reaction were compared based on the treatment groups. In the sites grafted with the test cement, bone degeneration characterized by loss of bone structure was seen and, in some samples, a chronic and/or purulent inflammation at low severity degrees was recorded. Purulent inflammation and bone degeneration were not noticed in the other two treatment groups. At 6 and 12 weeks, there was minimal or no irritation reaction in the BC and NC groups. In contrast, analysis of the cement sites revealed the presence of moderate tissue reaction at 6 weeks and slight reaction at 12 weeks, mainly due to bone degeneration, fibrosis, and purulent or chronic inflammation. Based on these results, the cement seems to act as moderate irritant to the bone and soft tissues. Nevertheless, in some samples at 3 and 6 weeks, new bone formed in intimate contact with the cement without interposition of soft tissues and presence of inflammatory reaction.

The percentages of new bone formed and residual graft material in the defects for the different treatment groups are shown in **Figure 10**.

All three groups showed a progressive increase of new bone fill throughout the time points investigated, with a significant increase in bone fill between 3 and 6 weeks, and 6 and 12 weeks. At 3 and 6 weeks, the NC group showed the highest amount of bone formed, whereas the cement group showed the lowest amount of new bone formation. At 12 weeks the amount of bone formed in the NC and cement group was not significantly different and both groups show significantly higher percentages of bone formation compared to BC group. However, the increase in new bone formation after 6 and 12 weeks in the cement group (15.427% and 62.282% respectively) needs to be carefully interpreted. In the specimens retrieved at 6 weeks in general, there was great variability, so a straightforward and conclusive analysis is difficult to conduct. At 6 weeks, not all the sites presented with visible graft in the region of interest (ROI), and indeed cement was seen in only 6 out of 12 sites grafted, while in the remaining 6 sites resorption and degeneration of host bone was visible with either no sign of cement or only remnants of cement present. At 12 weeks, only 1 site showed the presence of cement fully filling the ROI. In the sites where the cement was not visible (either at 6 and 12 weeks) the initial defect borders could no longer be defined. The defect outline was larger and filled with new woven bone. The histomorphometric measurements were therefore based upon the new defect borders. The increase in % of BA/TA in the defects treated with cement at 6 and 12 weeks can be explained by the larger ROI area considered and the fact that 62.3% of the area was now filled with new woven bone. If we consider the only sample that at 12 weeks still showed presence of the graft in situ, the BA/TA % was 12.46, increased compared to 3 weeks (as new bone was visible in contact with the perimeter of the graft) but significantly lower compared to the overall BA/TA % value obtained in the group (62.3%). This suggests that when space was available, new bone formed at faster rate and that the presence of the cement slowed down the new bone formation rate. However, the presence of the cement not only slowed down the bone

© 2024 The Authors. Advanced Functional Materials published by Wiley-VCH GmbH

16163028, 0, Downloaded from https://onlinelibrary.wiley.com/doi/10.1002/adfm.202401953 by Test, Wiley Online Library on [25/04/2024]. See the Terms and Conditions (https://onlinelibrary.wiley.com/terms-and-conditions) on Wiley Online Library for rules of use; OA articles are governed by the applicable Creative Commons License

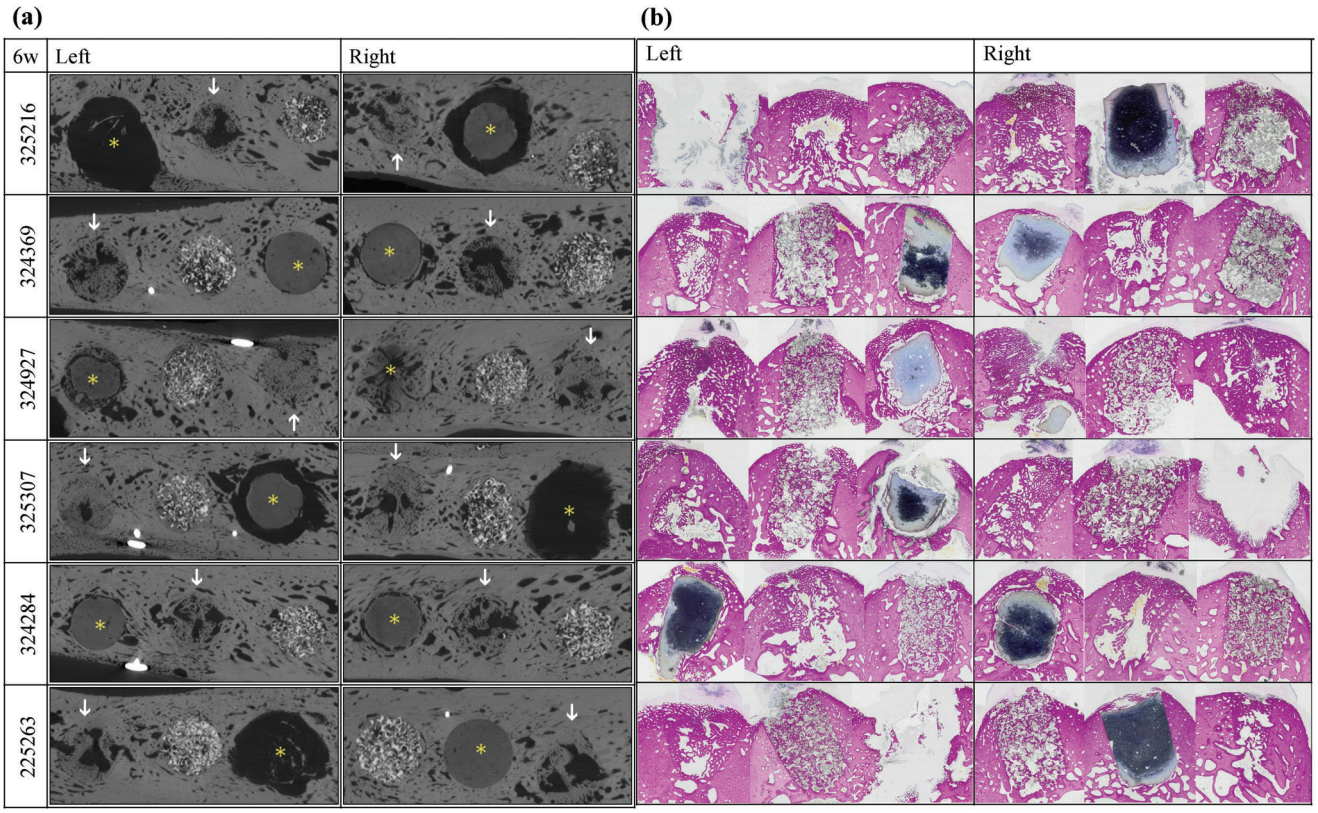

Figure 8. a) Axial view of XMT of samples at 6 weeks divided by left and right side of the mandible. Yellow asterisk: test cement; white arrow: NC; sites filled with particulate radiodense material (not marked): BC. b) Correspondent histological images of buccal lingual sections. Each animal is identified by a unique number (on the left column).

formation, but in some samples induced inflammation and host bone degeneration, which enlarged the defect outline. This was predominantly seen at 6 weeks. Between 6 and 12 weeks, new bone formed in these larger defects, with most of the cases completely filling the area with new woven bone.

The total amount of graft material reduced significantly for the cement group between 3, 6, and 12 weeks, while for the group treated with BC, it significantly reduced only after 12 weeks.

Whether the cement was completely resorbed or was ejected from the site between 3 and 6 weeks and 6 and 12 weeks is not clear. One hypothesis is that the presence of the cement induced an inflammatory response of the host tissue to the grafted material, which led to an initial delay in bone formation and degeneration of bone, which subsequently became infected. Bone destruction continued around the graft creating a sequestrated block of cement surrounded by necrotic bone. This possibly was discharged from the site through a sinus tract. The site (enlarged at this point) healed with new bone formation. This is likely to have happened between 3 and 6 weeks with new woven bone filling the enlarged defect between 6 and 12 weeks. However, this hypothesis does not explain why in other specimens the cement appeared to be gradually resorbed and integrated with the host bone. Another explanation is that the initial inflammatory response might have favored faster dissolution and resorption of the cement implanted. In some sites, this might have been more severe than others therefore not showing any trace of cement already at 6 weeks. The faster dissolution/resorption of the graft might have been favored by the acidic environment produced as a consequence of the inflammatory response.[49] The acidic environment can also activate osteoclasts and impair osteoblast differentiation and function leading to bone resorption.[50] Therefore graft resorption might have been too rapid to be balanced by new bone formation.

The initial inflammatory response might have been the result of a local tissue irritation due to exposure of the cement to the oral cavity (through a sinus tract) and possible colonization of the graft surface with bacteria. The release of components from the cement or a change in pH of the surrounding tissue due to the presence of the cement might have also contributed to the initial inflammatory response. The only component other than inorganic ions and elements ($Ca^{2+,}$ P, Na^{+}, and Si) released from the cement is a polymer polyvinylpyrrolidone (PVP). The amount of PVP used in the cement was low (0.33% by weight) and cell studies with conditioned media did not show signs of cytotoxicity after 7 days in culture, therefore the risk associated with the use of the polymer was considered negligible. PVP is also used in other commercially available bone grafts (Hydroset, Stryker, USA; NanoBone DBX Putty, Artoss GmbH, Germany). No safety concerns were raised in a previous preclinical study for a bone graft material containing PVP[51] while a different study showed that PVP was cytotoxic to human cervical carcinoma HeLa cells, inducing apoptosis.[52] However, they used much higher

© 2024 The Authors. Advanced Functional Materials published by Wiley-VCH GmbH

16163028, 0, Downloaded from https://onlinelibrary.wiley.com/doi/10.1002/adfm.202401953 by Test, Wiley Online Library on [25/04/2024]. See the Terms and Conditions (https://onlinelibrary.wiley.com/terms-and-conditions) on Wiley Online Library for rules of use; OA articles are governed by the applicable Creative Commons License

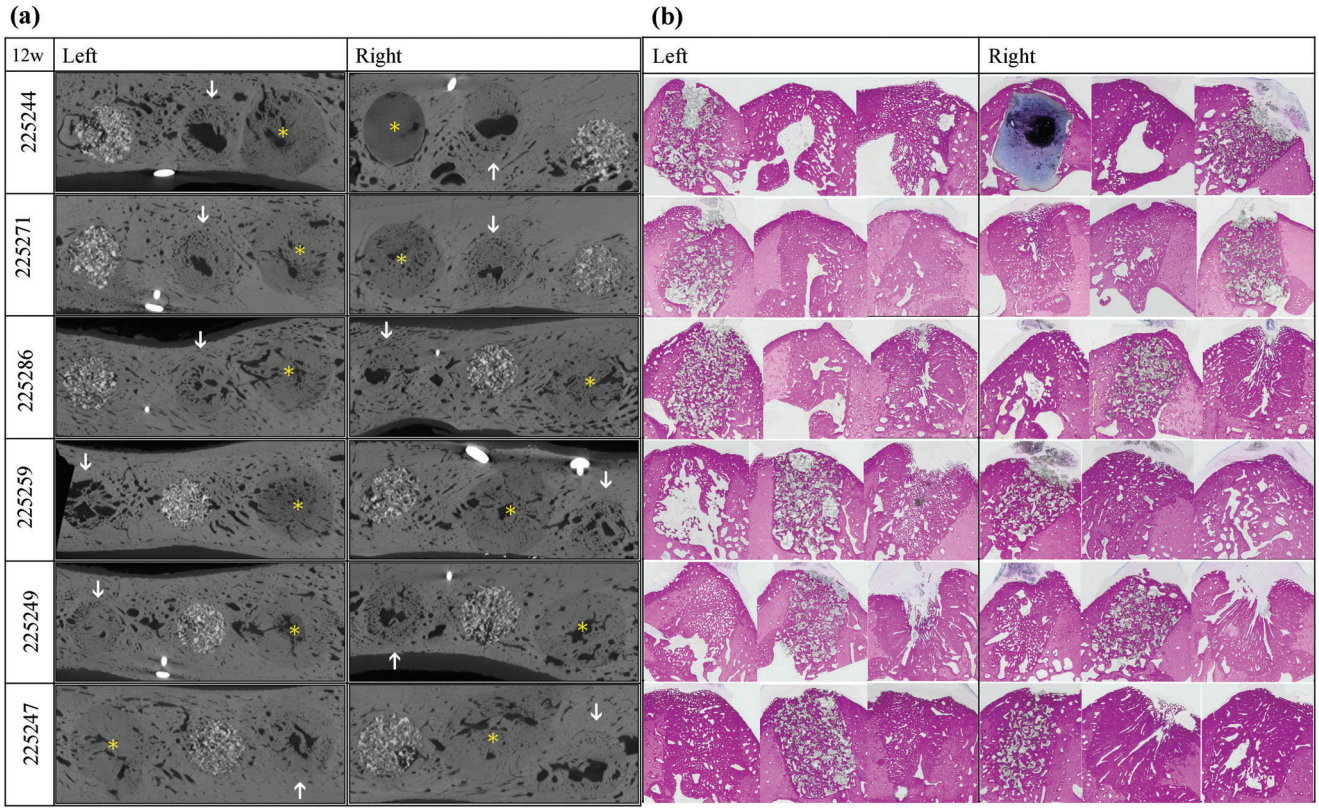

Figure 9. a) Axial view of XMT of samples at 12 weeks divided by left and right side of the mandible. Yellow asterisk: test cement; white arrow: NC; sites filled with particulate radiodense material (not marked): BC. b) Correspondent histological images of buccal lingual sections. Each animal is identified by a unique number (on the left column).

concentrations (from 2.5 to 20%, w/v) than that usually used in animal tests and concluded that although in vitro evidence of toxicity exists, animal and in vivo human studies showed that PVP is safe because lower concentrations are used.

Although in the present study a possible local irritation due to the release of PVP cannot be excluded, based on the analysis of the literature available and minimal doses used, it seems very unlikely that the results obtained can only be attributed to an inflammatory reaction against the PVP contained or released from the graft. Analysis of PVP release was not conducted and efforts should be made in the future to quantify the release in vitro. The irritation witnessed in the study is more likely due to a combination of factors, like change in pH of the surrounding environment due to the presence of cement, possible irritation due to PVP release or contact, communication with the oral cavity by a sinus tract that potentially increased the risk of bacteria colonization on the cement and lack of porosity within the graft. Lack of porosity was identified as an issue as most of the newly formed bone was found at the edge of the cement at all time points. This delayed bone formation due to insufficient space for blood vessels to grow within the graft and initiate bone healing.

Based on the high variability of the results a general conclusion on the performance of the material in vivo is difficult to achieve. Another limitation of this study is that a non-critical size defect was used and the anatomy of the defect was self-containing and self-healing as demonstrated with NC specimens. This surgical model was chosen as an initial step to prove the performance of test material as has been widely used by other investigators.[53,54] However, in the future efforts should be made to test the new graft material and its performance in a critical-size defect model.

3. Conclusion

This study used bioactive glass as a reagent in the setting reaction, dissolving and releasing ions that contributed to precipitation of the OCP and HA phases, demonstrating a novel way to produced CPCs. In vitro, the set cement promoted osteoblasts proliferation and resulted non cytotoxic.

The cement can be mixed and accurately injected through a delivery system, with setting times and mechanical strength compatible with clinical application. However, when applied to a preclinical model, the BG-CPC acted as a short-term moderate irritant with local inflammation and evidence of bone degeneration. Yet, at 12 weeks, all the cement had been replaced with new bone.

Based on the results of this study, we suggest that this novel cement has potential for use in dental bone grafting where an injectable product can be accurately placed to promote healing in a bone defect.

© 2024 The Authors. Advanced Functional Materials published by Wiley-VCH GmbH

16163028, 0, Downloaded from https://onlinelibrary.wiley.com/doi/10.1002/adfm.202401953 by Test, Wiley Online Library on [25/04/2024]. See the Terms and Conditions (https://onlinelibrary.wiley.com/terms-and-conditions) on Wiley Online Library for rules of use; OA articles are governed by the applicable Creative Commons License

16163028, 0, Downloaded from https://onlinelibrary.wiley.com/doi/10.1002/adfm.202401953 by Test, Wiley Online Library on [25/04/2024]. See the Terms and Conditions (https://onlinelibrary.wiley.com/terms-and-conditions) on Wiley Online Library for rules of use; OA articles are governed by the applicable Creative Commons License

(a)

Outcome	Endpoint	Parameter	Treatment Group		
			Cement	BC	NC
New Bone %	3 w	*n*	*12*	*12*	*12*
		Mean ± SD	0.617 ± 0.845	6.247 ± 4.090	13.00 4 ± 4.235
		Median	0.186	4.276	12.483
		(Q1-Q3)	(0.088 -1.177)	(3.097-8.990)	(9.131- 16.436)
	6 w	*n*	*9*	*12*	*11*
		Mean ± SD	15.427 ± 14.596	33.748 ± 5.757	51.830 ± 7.426
		Median (Q1-Q3)	10.713	35.673	51.102
			(5.5026- 23.002)	(31.108- 37.391)	(48.038-58.480)
	12 w	*n*	*10*	*12*	*11*
		Mean ± SD	62.282 ± 18.722	49.025 ± 5.668	63.295 ± 11.980
		Median (Q1-Q3)	68.641	48.087	67.680
			(58.727-73.034)	(44.777-52.309)	(58.375-73.192)
			Cement	BC	
Graft %	3 w	*n*	*12*	*12*	
		Mean ± SD	81.490 ± 26.001	34.184 ± 9.164	
		Median (Q1-Q3)	88.902	34.541	
			(84.585-92.0192)	(25.689-41.667)	
	6 w	*n*	*9*	*12*	
		Mean ± SD	43.0653 ± 26.057	32.679 ± 9.460	
		Median (Q1-Q3)	52.678 (	28.618	
			16.001-64.106)	(25.757 -38.642)	
	12 w	*n*	*10*	*12*	
		Mean ± SD	7.535 ± 22.236	21.448 ± 3.292	
		Median (Q1-Q3)	0.561	20.832	
			(0.198-0.878)	(18.871-23.550)	

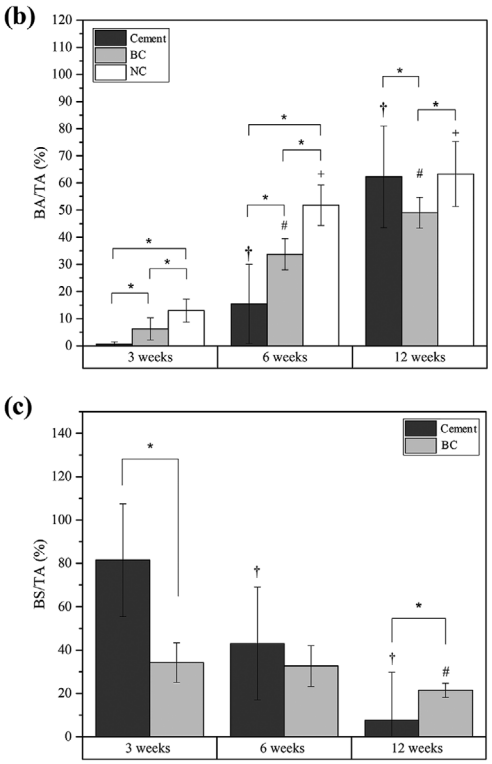

Figure 10. a) Descriptive statistics obtained from histomorphometric analysis categorized by treatment group and endpoint. b) % of Bone area/Tissue Area (BA/TA) of the different groups at each time point reported as mean ± SD. c) % of Bone Substitute/Tissue Area (BS/TA) for the different groups at different time points reported as mean ± SD, $n = 12$. A non- parametric Mann Whitney U test was employed to analyze the differences within the groups. Significance set at $p < 0.05$. ⁎: significant difference of the three group within the same time point; †: significant difference in group cement at the three different time points; #: significant difference in group BC at the three different time points; +:significant difference in group NC at the three different time points.

4. Experimental Section

Preparation of BG-CPC: The composition of the BG-CPC studied is shown in **Table 1**. The proportion of BG to calcium phosphate salts was chosen to give a Calcium to Phosphate ratio close to Octacalcium phosphate in order to promote its formation and subsequent HA formation. PVP was added to decrease the viscosity and induce greater fluidity in the cement.

The 2.5% Na_2HPO_4 solution was prepared by dissolving 7.5 g of Na_2HPO_4 salt in 300 ml of deionized water and stirring for 60 min until the solution was clear.

The raw materials for the cement powder were weighed using a calibrated analytical balance to obtain a batch of 50 g. They were then transferred in a 0.5 L glass jar and mixed in a Turbula Shaker mixer type T2F (Willy A. Bachofen AG, Basel, Switzerland) at 49 rpm for 20 min. Packaging of raw materials was conducted externally by Blispac (Balagny Sur Thérain, France): 1.3 g of the mixed cement powder was loaded in mixing and delivery devices (Medmix P-system, MEDMIX Systems AG, Switzerland) and 0.71 ml of 2.5% Na_2HPO_4 solution was added into 1 ml syringes (BD Luer-Lok, BD, USA) and the packaged products sent for gamma irradiation (^{60}Cobalt source of irradiation in the range of 25 to 40 kGy Synergy Health Marseille, France). Characterization of raw materials by XRD and FTIR can be found in Section S1 (Supporting Information).

Characterization of Properties of BG-CPC: Initial and final setting times were assessed using the Gilmore needle test according to ASTM C266-89.[55] Five packaged and irradiated cement samples were assessed.

Table 1. Composition of the BG-CPC. Liquid to powder ratio: 0.55 ml g^{-1}.

Raw material	Formula	Wt.%	Supplier
Powder			
Bioactive glass	42.0 SiO_2, 4.0 P_2O_5, 39.0 CaO, 15.0 Na_2O (mol%)	63.99	Noraker
Monocalcium Phosphate (Anhydrous)	$Ca(H_2PO_4)_2$	7.87	Innophos
Monocalcium Phosphate (Monohydrate)	$Ca(H_2PO_4)_2.H_2O$	27.81	Innophos
Polyvinylpyrrolidone	$(C_6N_9NO)_n$	0.33	Ashland
Liquid			
Disodium hydrogen phosphate	Na_2HPO_4	2.5%	Innophos

© 2024 The Authors. Advanced Functional Materials published by Wiley-VCH GmbH

For the immersion studies cements were mixed within the mixing device (Section S3, Supporting Information) for 30 s and the cement paste produced was loaded in cylindrical steel molds (6 mm height x 4 mm diameter) between 2 steel plates clamped together using a G clamp and placed into a 37 ± 1 °C oven. After 120 min the clamp and plates were removed and the steel molds containing the samples were abraded against a silicon-carbide paper (Norton, P400) to remove excess cement and ensure flat plane parallel surfaces at the top and bottom of the cylinders. The set cement cylinders were then immersed in 10 ml of Tris buffer solution and 10 ml of SBF and stored in a shaking 37 ± 1 °C oven at 60 rpm, for 1 h, 1 day, 7 day or 28 days ($n = 8$ samples for each ageing solution and each time point). Tris buffer was prepared by dissolving 15.090 g of tris(hydroxymethyl)aminomethane (Sigma Aldrich, UK) in 800 ml of deionized water. 44.2 ml 1 M HCl (Sigma Aldrich, UK) was then added, and the solution was heated to 37 °C overnight. The pH of the solution was then adjusted to 7.34 by slowly adding 1 M HCl and monitoring the pH change with a pH meter (Oakton Instruments, Nijkerk, The Netherlands). The volume of the solution was then adjusted to 2 L by adding deionized water.

SBF was prepared based on Kokubo's recipe:15.992 g of NaCl, followed by 0.70 g of $NaHCO_3$, 0.448 g of KCl, 0.456 g of $K_2HPO_4.3H_2O$, 0.610 g of $MgCl_2.6H_2O$, 70 mL of 1.0 M HCl, 0.736 g of $CaCl_2.2H_2O$, 0.132 g of Na_2SO_4 and 12.114 g of Tris (all Sigma-Aldrich) were slowly dissolved one after the other in 1500 ml of deionized water kept at 37 °C.[56] To prevent bacterial contamination 0.4 g of NaN3 was added to the solution. The pH of the solution was then adjusted with 1 M HCl to reach a value of 7.4 at 37 °C and the volume adjusted with deionized water to obtain a 2 L solution.

After immersion the cements were removed from the ageing solution and characterized for compressive strength, composition of crystal phases formed using XRD and FTIR, microstructure by SEM, and ion release by ICP-OES.

Compressive strength was measured with an Instron 5567 mechanical property testing machine (Instron, High Wycombe, UK) with a 1 kN load cell. Force was applied at a crosshead displacement rate of 1 mm min^{-1} until fracture. Eight specimens were tested for each time point and each immersion solution.

For the analysis of crystal phases formed XRD and FTIR were used. XRD was conducted using an XPert Pro X-ray diffractometer (Panalytical, The Netherlands) with a CuKα radiation operating at 45 kV/40 mA, in the 2θ range of 3°–70° with a step size of 0.001 °2θ. FTIR was conducted using a Frontier IR/FTIR Spectrometer (PerkinElmer, Waltham, MA, USA) in attenuated total reflectance (ATR) mode and data were collected from 4000 to 500 cm^{-1}, with 10 scans per sample and resolution of 4 cm^{-1}. One sample for each solution and immersion time was tested for both techniques.

The fracture surfaces of the cement cylinders were examined under SEM to evaluate morphology of the crystal phases formed. Specimens were gold coated using an automatic sputter coater (SC7620, Quorum Technologies, UK). Photomicrographs were taken using a Scanning Electron Microscope (FEI Inspect F, Oxford Instruments, UK) with the accelerating voltage of 2 kV.

ICP-OES Varian Vista-PRO CCD was used to detect the concentrations of calcium, sodium, phosphorous, and silicon after immersion of the samples in Tris and SBF solutions. Samples were diluted by a factor of 10 and 100 (the latter for measuring the Na^+ concentration in SBF immersed samples) with deionized water and were acidified by using nitric acid (69%, VWR, Radnor, PA, USA) to obtain a 2% solution. Ion concentrations were measured against a range of prepared multi-element standard solutions (Si, Ca, Na, P; VWR, Radnor, PA, USA) from 0 to 80 ppm prepared with deionized water and 2% nitric acid. Three solutions for each immersion point and cement composition were measured.

Cell culture studies were performed to evaluate the effect of the BG-CPC on viability, proliferation, and differentiation of MC3T3-E1 osteoblast cells (European Collection of Cell Cultures) using liquid extracts of the material (conditioned medium). The test material was prepared by immersing a cylindrical cement sample in 10 ml of Minimum Essential Medium Eagle Alpha Modification (α-MEM, Lonza, Switzerland) and stored in a shaking incubator (60 rpm) at 37 °C for 24 h. Then the extract of the test material was aseptically decanted, filter sterilized (pore size 0.2 µm), and supplemented with 10% fetal bovine serum (FBS), 1% *L*-glutamine, and 1% penicillin/streptomycin. To control the activity of the conditioned media, a negative and a positive control sample were run in parallel with the test material. For the negative control (NC), cells were incubated with α-MEM supplemented with 10% FBS, 1% *L*-glutamine, and 1% penicillin/streptomycin. As a positive control a solution of 0.1 mg ml^{-1} sodium lauryl sulphate (SLS, Sigma Aldrich, UK) in α-MEM was prepared and is known to be toxic under the test conditions.

To assess cytotoxicity of cement conditioned medium, MC3T3-E1 cells were seeded in a 96 well microtiter plate at a concentration of 5×10^3 cells/well in 100 µl of α-MEM supplemented with 1% penicillin/streptomycin, 1% *L*-glutamine and 2% FBS. 100 µl of α-MEM was used in the peripheral wells of the plate (blanks). Cells were incubated for 24 h to allow adherence and formation of a semi-confluent layer. After 24 h, the culture medium was aspirated and 100 µl of conditioned medium, NC solution or SLS solution was added in the respective wells. For each experimental group six wells were used. Cells were then incubated for 1 day and 7 days, changing the medium every two days with the appropriate conditioned or normal media. After 1 day and 7 days, plates were evaluated under a light microscope to examine growth characteristics of control and treated cells. The culture medium was then aseptically discarded and 50 µl of MTT solution was added to each well. The MTT solution was prepared by adding thiazolyl blue tetrazolium bromide (Sigma Aldrich, UK) in pure α-MEM at a concentration of 1 mg ml^{-1}. The solution was filter sterilized (pore size 0.2 µm) before being added to the wells. Plates were further incubated for 2 h at 37 °C and 5% CO_2 atmosphere. Then the MTT solution was discarded and 100 µl of 2-isopropanol was added in each well to solubilize any formazan crystals formed. The intensity of purple colored reaction product was quantified by measuring the absorbance spectra at 570 nm using an Optima plate reader (BMG Labtech, Germany). The average absorbance of the blanks was subtracted from the absorbance values of test and control wells. Cell viability was calculated using the equation below:

$$\text{Cellviability} = (\text{OD (test)} / \text{(OD (control))} \times 100 \quad (9)$$

where OD (test) corresponds to the optical density of the experimental medium and OD (control) corresponds to that of the NC. Data from NC were used as 100% cell viability and were compared against experimental data. Three independent experiments for each time point were performed for assessing reproducibility. Results were presented as mean±SD % cell viability normalized against the NC.

For cell proliferation, a DNA assay using the fluorochrome bisbenzimide Hoechst 33258 was used. Cells were prepared as for the MTT test described above and treated with conditioned medium and NC for 1 day and 7 days, exchanging the medium every two days.

After each time point the medium was removed, wells were washed with PBS, emptied and plates stored at −20 °C for at least 24 h. Then plates were removed from the freezer and allowed to thaw at room temperature. 100 µl of deionized water was added in each well and plates were returned to −20 °C for 1 h to rupture the cell membranes and release the DNA. The resulting lysate was then incubated with 100 µl of fluorochrome bisbenzimide Hoechst 33258 solution (20 µg ml^{-1} in TNE buffer with 10 mM Tris, 1 mM EDTA, and 2 M NaCl at pH 7.4). The resultant fluorescence intensity was measured in a plate reader at 355 nm excitation and 460 nm emission. The average fluorescence intensity of the blanks was subtracted from the fluorescence intensities of test and control wells. Three independent experiments for each time point were performed. Results were presented as mean±SD.

For the cell differentiation assay, ALP activity of MC3T3-E1 cells was studied. Cells were seeded and treated MTT studies described above for 7 days. After 7 days cells were washed with PBS and wells emptied and stored at −20 °C. When all plates were ready for use, they were thawed and 100 µl of working solution was added to each well and incubated at 37 °C for 45 min. Working solution was prepared by using 8 ml Tris buffer solution, 15 µl 2 M $MgCl_2$ and 20 mg 4-Nitropheyl phosphate disodium salt hexahydrate (all Sigma Aldrich) to obtain a

© 2024 The Authors. Advanced Functional Materials published by Wiley-VCH GmbH

16163028, 0, Downloaded from https://onlinelibrary.wiley.com/doi/10.1002/adfm.202401953 by Test, Wiley Online Library on [25/04/2024]. See the Terms and Conditions (https://onlinelibrary.wiley.com/terms-and-conditions) on Wiley Online Library for rules of use; OA articles are governed by the applicable Creative Commons License

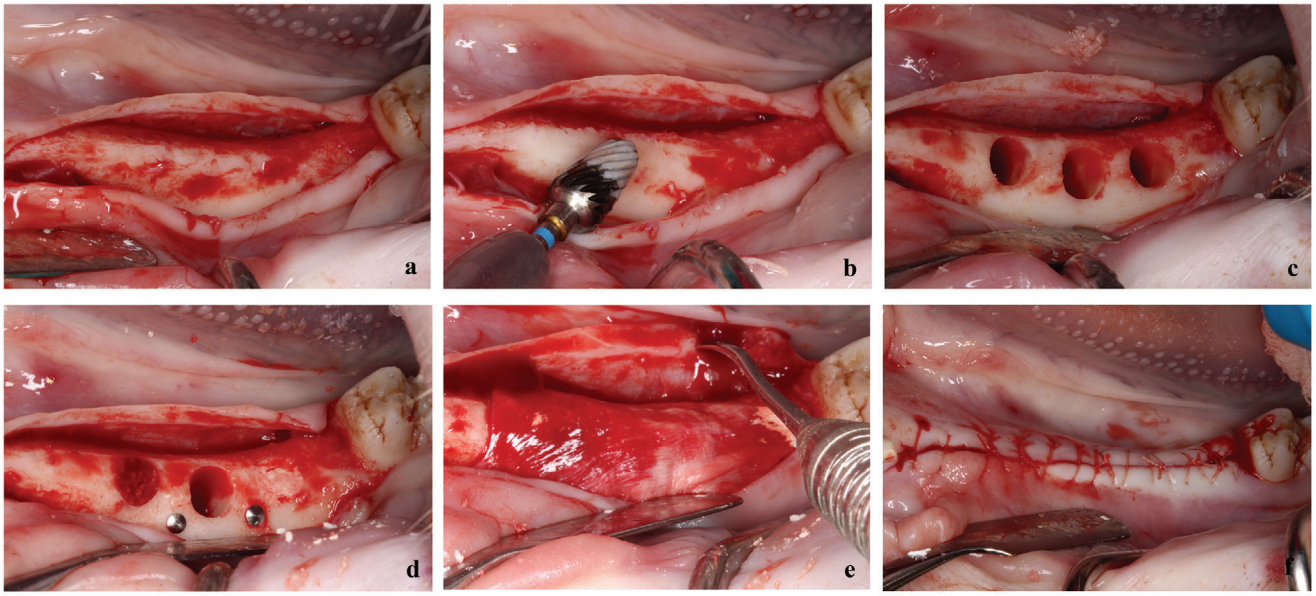

Figure 11. Clinical images showing the steps involved in the second surgery. a): Incision of the edentulous area; b): flattening of the alveolar ridge exposed; c): creation of surgical defects (6×6 mm); d): from left to right defect filled Bone Ceramic, empty defect, defect filled with the test cement; e): defects covered by collagen membrane (BioGide); f): wounds sutured.

2.5 mg ml^{-1} 4-Nitropheyl phosphate disodium salt hexahydrate solution. After incubation, 0.5 M NaOH was used to stop the reaction, and the intensity of yellow color produced was evaluated measuring the absorbance at 405 nm in a plate reader (reaction product *p*-Nitrophenol, indicative of ALP enzymatic action). The average absorbance of the blanks was subtracted from the absorbance values of test and control wells. Three independent experiments for each time point were performed. Results were presented as mean±SD.

Animal Study: The study design with invasive procedures was based on the requirements described in ISO 10993–6 and approved by the ethical committee of the University of Lund, Sweden (Approval number: M-192-14). A total of 18 adult Gottingen female minipigs (Ellegaard, Denmark) with an average body weight of 44 Kg were used. General anesthesia was initiated and maintained by i.m. injection of ketamine 50 mg ml^{-1} and midazolam 5 mg ml^{-1}. After administration of local anesthesia (2% xylocaine with 1:100 000 adrenaline) buccal and lingual full-thickness mucoperiosteal flaps were raised bilaterally in the mandible and lower premolars P2, P3, P4, and first molar M1 were extracted. The flaps were sutured with single Vicryl 4-0 to achieve primary closure. The animals received antibiotics for 5 days postoperatively (Streptocillin vet 3–4 ml/animal i.m., a combination of streptomycin and benzylpenicillin) and painkillers for 3 days postoperatively (Temgesic 3–5 ml/animal i.m., buprenorphine). After 3 months of healing, using the same anesthesia regime as described above, alveolar crestal incisions were made in the edentulous area and bucco-lingual full-thickness flaps were raised bilaterally. The alveolar ridge was flattened out with a rotary bur to obtain a width of at least 8 mm. For the surgical model, three cylindrical standardized bony defects were created in the alveolar bone in each side of the mandible (a total of six defects for each animal) by using a series of implant drills (Straumann Guided Instruments) to achieve cylindrical defects of 6 mm in final depth and width. Titanium tacks (Titan pin set, 3 mm, Botiss, Germany) were inserted on either side of the central defect to help in the identification of the defects for histological processing. Each animal received two test materials (BG-CPC), two positive controls (Bone Ceramic, BC, Straumann AG: biphasic calcium phosphate ceramic 60% HA/40% β-TCP with particle size ranging between 500–1000 µm) and two negative controls (NC: defect unfilled). Allocation was randomized by a computer-generated randomization procedure. Following grafting the defects were covered with a collagen membrane (Bio-Gide, Geistlich Biomaterials, Switzerland) and the flaps closed with single 4-0 Vicryl sutures (**Figure 11**). The animals received antibiotics for 5 days postoperatively and painkillers for 3 days postoperatively as described above. After 3, 6, and 12 weeks of healing, six animals for each time point were euthanized by an intravenous injection of 20% solution of pentobarbital. Mandibles were dissected, hemisected and the samples were fixed in 4% formaldehyde solution for 2 weeks.

Prior to histological processing, the hemimandible block containing the three defects was examined using an in-house-built X-Ray Microtomography (XMT) system (MuCAT 2, QMUL, G.R. Davis, UK). Samples were X-rayed at 90 kV, 180 µA, and with a 1.2 mm copper and aluminum filter to obtain 3D images (voxel size 40 µm) which were visualized using Tomview software (QMUL, G.R. Davis, UK). The XMT slices here presented were deliberately chosen to match the histological sections in order to facilitate subsequent analysis.

Histomorphometric and histopathological analysis were conducted at *AnaPath GmbH* (Liestal, Switzerland). The samples were dehydrated in ascending concentrations of ethanol and xylene, infiltrated, and embedded in methyl methacrylate. Each defect was cut in a bucco-lingual direction in the middle of the defect. One section per defect was obtained, ground, and polished to a final thickness of 50 µm and stained with Paragon. The region of interest (ROI) was defined as the full extent of each defect where the upper line defined the outermost rim of the bone trabeculae on the top of the alveolar ridge (Section S4, Supporting Information). Photographs were taken using an Olympus BX43 light microscope integrated with an Olympus XC30 camera. Image analysis was performed using Olympus cellSens microimaging software (Olympus Life Science, UK).

Outcome parameters from histomorphometric analysis were summarized in terms of means and standard deviations. The histopathological examination was carried out using a semi-quantitative scoring system adapted from ISO 10993–6:2016(E).

Statistical Analysis: Data analysis was performed using OriginPro 2016 (OriginLab, Northampton, MA). The Shapiro–Wilk test was used to assess normality of distribution within each group for both cell culture studies and histomorphometric analysis. A non- parametric Mann Whitney U test was employed to analyze the differences within the groups for the MTT assay at 1 day and the histomorphometric analysis. An unpaired *t*-test was used to analyze the differences within the groups for the MTT assay at

© 2024 The Authors. Advanced Functional Materials published by Wiley-VCH GmbH

16163028, 0, Downloaded from https://onlinelibrary.wiley.com/doi/10.1002/adfm.202401953 by Test, Wiley Online Library on [25/04/2024]. See the Terms and Conditions (https://onlinelibrary.wiley.com/terms-and-conditions) on Wiley Online Library for rules of use; OA articles are governed by the applicable Creative Commons License

7 days, the DNA assay, and ALP assay. Statistical significance was set at $p < 0.05$. Results are presented as means ± SD.

Supporting Information

Supporting Information is available from the Wiley Online Library or from the author.

Acknowledgements

This work was funded by the Medical Research Council (reference project number: MR/M025306/1).

Conflict of Interest

The authors declare no conflict of interest

Data Availability Statement

The data that support the findings of this study are available from the corresponding author upon reasonable request.

Keywords

bioactive glasses, bone graft, bone regeneration, calcium phosphate cements

Received: January 31, 2024
Revised: March 18, 2024
Published online:

[1] R. Zhao, R. Yang, P. R. Cooper, Z. Khurshid, A. Shavandi, J. Ratnayake, *Molecules* **2021**, *26*, 3007.
[2] P. Giannoudis, J. C. Arts, G. Schmidmaier, S. Larsson, *Injury* **2011**, *42*, S1.
[3] S. S. Jensen, N. Broggini, E. Hjørting-Hansen, R. Schenk, D. Buser, *Clin Oral Implants Res* **2006**, *17*, 237.
[4] R. J. Miron, *Periodontol. 2000* **2023**, https//:doi.org/10.1111/prd.12517.
[5] R. J. Miron, Y. F. Zhang, *J Dent Res* **2012**, *91*, 736.
[6] V. Chappuis, L. Rahman, R. Buser, S. Janner, U. C. Belser, D. Buser, *J Dent Res* **2018**, *97*, 266.
[7] B. K. Tay, V. V. Patel, D. S. Bradford, *Orthop Clin North Am* **1999**, *30*, 615.
[8] S.-Y. Kim, Y.-J. Lee, W.-T. Cho, S.-H. Hwang, S.-C. Heo, H.-J. Kim, J.-B. Huh, *Materials* **2021**, *14*, 4464.
[9] H. Nowzari, C. Teoh, A. E. Rodriguez, *J Indian Soc Periodontol* **2022**, *26*, 178.
[10] B. Wessing, S. Lettner, W. Zechner, *Int. J. Oral. Maxillofac Implants* **2018**, *33*, 87.
[11] L. L. Hench, *J. Mater. Sci.-Mater. Med.* **2006**, *17*, 967.
[12] P. Valerio, M. M. Pereira, A. M. Goes, M. F. Leite, *Biomaterials* **2004**, *25*, 2941.
[13] I. D. Xynos, A. J. Edgar, L. D. K. Buttery, L. L. Hench, J. M. Polak, *J. Biomed. Mater. Res.* **2001**, *55*, 151.
[14] R. M. Day, *Tissue Eng.* **2005**, *11*, 768.
[15] A. Hoppe, N. S. Güldal, A. R. Boccaccini, *Biomaterials* **2011**, *32*, 2757.
[16] I. Allan, H. Newman, M. Wilson, *Biomaterials* **2001**, *22*, 1683.
[17] L.-E. Monfoulet, P. Becquart, D. Marchat, K. Vandamme, M. Bourguignon, E. Pacard, V. Viateau, H. Petite, D. Logeart-Avramoglou, *Tissue Eng., Part A* **2014**, *20*, 1827.
[18] T. R. Arnett, *J. Nutr.* **2008**, *138*, 415S.
[19] A. A. El-Rashidy, J. A. Roether, L. Harhaus, U. Kneser, A. R. Boccaccini, *Acta Biomater.* **2017**, *62*, 1.
[20] J. Chen, L. Zeng, X. Chen, T. Liao, J. Zheng, *Bioact Mater* **2018**, *3*, 315.
[21] F. E. Ciraldo, E. Boccardi, V. Melli, F. Westhauser, A. R. Boccaccini, *Acta Biomater.* **2018**, *75*, 3.
[22] B. L. Eppley, W. S. Pietrzak, M. W. Blanton, *J. Craniofac. Surg.* **2005**, *16*, 981.
[23] S. V. Dorozhkin, *J. Mater. Sci.* **2008**, *43*, 3028.
[24] D. Ambard, P. Swider, *Eur. J. Mech. A Solids* **2006**, *25*, 927.
[25] R. Krüger, J. Groll, *Biomaterials* **2012**, *33*, 5887.
[26] J. Zhang, W. Liu, V. Schnitzler, F. Tancret, J.-M. Bouler, *Acta Biomater.* **2014**, *10*, 1035.
[27] A. W. Barone, S. Andreana, R. Dziak, *Med. Res. Arch.* **2020**, *8*.
[28] S. Larsson, G. Hannink, *Injury* **2011**, *42*, S30.
[29] N. W. Kent, R. G. Hill, N. Karpukhina, *Mater. Lett.* **2016**, *162*, 32.
[30] L. L. Hench, *J. Mater. Sci.: Mater. Med.* **2006**, *17*, 967.
[31] a) D. M. Reffitt, N. Ogston, R. Jugdaohsingh, H. F. J. Cheung, B. A. J. Evans, R. P. H. Thompson, J. J. Powell, G. N. Hampson, *Bone* **2003**, *32*, 127; b) S. Maeno, Y. Niki, H. Matsumoto, H. Morioka, T. Yatabe, A. Funayama, Y. Toyama, T. Taguchi, J. Tanaka, *Biomaterials* **2005**, *26*, 4847.
[32] J. C. Elliott, Structure and chemistry of the apatites and other calcium orthophosphates, Elsevier, **2013**.
[33] L. Bingel, D. Groh, N. Karpukhina, D. S. Brauer, *Mater. Lett.* **2015**, *143*, 279.
[34] E. Fernandez, F. J. Gil, M. P. Ginebra, F. C. M. Driessens, J. A. Planell, S. M. Best, *J. Mater. Sci.: Mater. Med.* **1999**, *10*, 169.
[35] N. W. Kent, Development of a Novel In-vivo Setting Bone Graft Substitute From Bioactive Glass (Doctoral dissertation, Queen Mary University of London), **2014**.
[36] F. C. M. Driessens, M. G. Boltong, O. Bermudez, J. A. Planell, M. P. Ginebra, E. Fernandez, *J. Mater. Sci.: Mater. Med.* **1994**, *5*, 164.
[37] L. C. Chow, E. D. Eanes eds.,*Octacalcium phosphate (Vol. 18). Karger Medical and Scientific Publishers*, Karger, Basel **2001**.
[38] W. E. Brown, N. Eidelman, B. Tomazic, *Adv. Dent. Res.* **1987**, *1*, 306.
[39] F. F. Abraham, G. M. Pound, *J. Chem. Phys.* **1968**, *48*, 732.
[40] J. J. De Yoreo, P. G. Vekilov, *Rev Mineral Geochem* **2003**, *54*, 57.
[41] R. Z. Legeros, O. R. Trautz, J. P. Legeros, E. Klein, W. P. Shirra, *Science* **1967**, *155*, 1409.
[42] W. E. Brown, J. P. Smith, J. R. Lehr, A. W. Frazier, *Nature* **1962**, *196*, 1050.
[43] M. P. Ginebra, E. Fernandez, M. G. Boltong, J. A. Planell, O. Bermudez, F. C. M. Driessens, *Bioceramics* **1994**, *7*, 273.
[44] N. W. Kent, G. Blunn, N. Karpukhina, G. Davis, R. F. de Godoy, R. M. Wilson, M. Coathup, L. Onwordi, W. Y. Quak, R. Hill, *J. Biomed. Mater. Res., Part B* **2018**, *106*, 21.
[45] L. C. Chow, S. Hirayama, S. Takagi, E. Parry, *J. Biomed. Mater. Res.* **2000**, *53*, 511.
[46] M. Bohner, *Injury* **2000**, *31*, D37.
[47] F. Theiss, D. Apelt, B. Brand, A. Kutter, K. Zlinszky, M. Bohner, S. Matter, C. Frei, J. A. Auer, B. Von Rechenberg, *Biomaterials* **2005**, *26*, 4383.
[48] D. R. Marsh, G. Li, *Br. Med. Bull.* **1999**, *55*, 856.
[49] R. P. F. Lanao, S. C. G. Leeuwenburgh, J. G. C. Wolke, J. A. Jansen, *Biomaterials* **2011**, *32*, 8839.

© 2024 The Authors. Advanced Functional Materials published by Wiley-VCH GmbH

16163028, 0, Downloaded from https://onlinelibrary.wiley.com/doi/10.1002/adfm.202401953 by Test, Wiley Online Library on [25/04/2024]. See the Terms and Conditions (https://onlinelibrary.wiley.com/terms-and-conditions) on Wiley Online Library for rules of use; OA articles are governed by the applicable Creative Commons License

[50] G.-H. Lee, J.-D. Hwang, J.-Y. Choi, H.-J. Park, J.-Y. Cho, K.-W. Kim, H.-J. Chae, H.-R. Kim, *Int. J. Biochem. Cell Biol.* **2011**, *43*, 1305.
[51] M. Dau, C. Ganz, F. Zaage, B. Frerich, T. Gerber, *Int. J. Nanomed.* **2017**, *12*, 7393.
[52] Y.-B. Wang, Y. Lou, Z.-F. Luo, D.-F. Zhang, Y.-Z. Wang, *Biochem. Biophys. Res. Commun.* **2003**, *308*, 878.
[53] C. Dahlin, M. Obrecht, M. Dard, N. Donos, *Clin Oral Implants Res* **2015**, *26*, 814.
[54] I. Mihatovic, F. Schwarz, K. Obreja, J. Becker, R. Sader, M. Dard, G. John, *Clin Oral Investig* **2020**, *24*, 3289.
[55] I. ASTM International, **2018**.
[56] T. Kokubo, H. Takadama, *Biomaterials* **2006**, *27*, 2907.

© 2024 The Authors. Advanced Functional Materials published by Wiley-VCH GmbH

16163028, 0, Downloaded from https://onlinelibrary.wiley.com/doi/10.1002/adfm.202401953 by Test, Wiley Online Library on [25/04/2024]. See the Terms and Conditions (https://onlinelibrary.wiley.com/terms-and-conditions) on Wiley Online Library for rules of use; OA articles are governed by the applicable Creative Commons License